PAPER

Check for updates

In vivo detection of salicylic acid in sunflower seedlings under salt stress†

Ye Hu,[ab] Jing Zhao,[ac] Haiyang Li,[a] Xiaodong Wang,[ab] Peichen Hou,[ab] Cheng Wang,[ab] Aixue Li [ID] *[ab] and Liping Chen*[ab]

Salicylic acid (SA) is an important phytohormone. It plays an essential role in regulating many physiological processes of plants. Most of the conventional methods for SA detection are based on *in vitro* processes. More attention should be paid to develop *in vivo* methods for SA detection. In this work, Pt nanoflowers and GO were simultaneously electrodeposited and reduced on a Pt wire microelectrode in one step. The Pt nanoflowers/ERGO modified Pt microsensor demonstrated high sensitivity and selectivity for SA. SA could be detected from 100 pM to 1 μM with a detection limit of 48.11 pM. Then this microsensor was used to detect SA in the stem of sunflower seedlings under different salt stresses *in vivo*. The result showed that with the increasing concentration of salt, SA levels decreased. Our result was also confirmed by UPLC-MS and gene expression analysis. To the best of our knowledge, this is the first report of *in vivo* detection of SA in plants using the Pt nanoflowers/ERGO modified Pt microelectrode. It is foreseeable that our strategy could pave the way for the *in vivo* detection of phytohormones in plants.

1. Introduction

Salicylic acid (SA) is an important phytohormone, which widely exists in both monocot and dicot plants.[1] As a signal molecule, it plays an essential role in regulating many physiological processes of plants, including flowering, seed germination, heat production, membrane permeability, defence responses, *etc.*[2] The level of SA varies from ng to mg per gram of fresh weight in different plant species, and it will change under biotic and abiotic stresses for enhancing plants stress toleration.[3]

Further studies on the synthesis, transport and molecular mechanisms of SA require the accurate quantitative analysis of SA. Nowadays, there are many technologies for detecting SA level in plants, such as high performance liquid chromatography (HPLC),[4] gas chromatography-mass spectrometry (GC-MS),[5] enzyme linked immunosorbent assay (ELISA) and fluorescence spectrometry[6,7] *etc.* But in these methods, SA is measured *in vitro* using plant samples, such as roots, stems and leaves. The plant samples need to undergo complex pre-processing, where complex and expensive instruments are

always required, and some biological information may be lost during this process. In addition, the collections of plant samples always result in great damage and even death, while many plant materials are very precious and rare. More importantly, an *in vivo* detection of SA would provide more instant and accurate information about the response mechanism of plants under different environmental conditions. Therefore, it is very important to develop *in vivo* method for the detection of SA.

To date, there are only a few reports for the *in vivo* detection of SA, such as colorimetry,[8] bioluminescence,[9] reverse iontophoresis[10] and electrochemical sensors.[11] Colorimetry and bioluminescence methods were mainly used to map the spatial distribution of SA in plant tissues. Reverse iontophoresis has been used to assay the level of SA in basil leaves *in situ*, but it needed an 8 hours extraction period for collecting the sap of the plants, which couldn't reflect the instant information of SA under changed environment. Sun *et al.*[11] detected the change of SA in tomato leaves *in vivo* using a paper-based electrochemical sensor, which indicated that electrochemical sensor could be used for *in situ* and *in vivo* detection of SA in plants. However, it seems that this sensor is more suitable for the leaves, while not suitable for the stems or roots of the plants.

In recent years, microelectrode has attracted much interest due to its unique characters, such as smaller size, rapid response time, increased signal-to-noise ratio, and less requirement for support electrolyte, *etc.*[12,13] Additionally, the small size of microelectrode makes it ideal for *in vivo* application in plants, especially for the stems or roots of plants. For example, Pt microelectrode has been successfully used to monitor the H_2O_2,[14–17] NO and pH[15] in plants *in vivo*. However,

[a]*Beijing Research Center of Intelligent Equipment for Agriculture, Beijing Academy of Agriculture and Forestry Sciences, Beijing 100097, P. R. China. E-mail: liax@nercita.org.cn*

[b]*Beijing Research Center for Information Technology in Agriculture, Beijing Academy of Agriculture and Forestry Sciences, Beijing 100097, P. R. China. E-mail: chenlp@nercita.org.cn*

[c]*Department of Environmental Science and Engineering, Zhejiang Ocean University, Zhoushan, Zhejiang 316022, P. R. China*

up to date, there are few reports about the application of microelectrode in detecting of phytohormone in plants *in vivo*.

As the environment for *in vivo* detection is very complex, complicated and complex method for fabrication of the micro-sensor is not suitable. It has been reported that electrochemically reduced graphene oxide (ERGO)–metal nanocomposite films can be obtained by direct electrodeposition method.[18,19] This method is green and fast, and the prepared nanocomposite films exhibit excellent catalytic activity. In this work, Pt nanoflowers (PtNF) and ERGO were successfully fabricated on a Pt wire microelectrode by one step electrodeposition method. Then this PtNF/ERGO modified Pt microelectrode was used to detect SA in the stem of sunflower seedlings under salt stress *in vivo*. To the best of our knowledge, this is the first report for *in vivo* detection of SA in plants using the PtNF/ERGO modified Pt microelectrode. It may open the opportunity for application of microelectrode in detecting of phytohormone *in vivo* in plants. Our result was also confirmed by UPLC-MS and gene expression analysis.

2. Materials and methods

2.1. Chemicals and materials

Hexachloroplatinic acid hexahydrate ($H_2PtCl_6 \cdot 6H_2O$), SA, methyl jasmonate, malic acid, succinic acid, citric acid, indole acetic acid and abscisic acid were purchased from Sigma-Aldrich Co. LLC. The monolayer graphene oxide (GO) (diameter: 500 nm to 5 μm) was obtained from Nanjing XFNANO Materials Tech Co. Ltd. All other chemicals used were analytically grade and purchased from Beijing Chemical Works. All aqueous solutions were prepared with ultrapure water. The SA stock solution (0.01 M) was dissolved by 0.01 M PBS (pH = 7.0) with 0.2% ethanol. It was stored under 4 °C and diluted freshly by PBS before use.

2.2. Preparation of the Pt nanoflowers/ERGO modified Pt (PtNF/ERGO/Pt) microelectrodes

Pt wire microelectrode (0.5 mm in diameter) was purchased from Tianjin Ida Heng Sheng Technology Development Co., Ltd (Tianjin, China). The microelectrode was immersed in concentrated nitric acid solution for 10 min to remove the impurities. Then, it was polished in turn with 0.3 and 0.05 μm alumina powder, and ultrasonic cleaning with deionized water and ethanol. After drying by N_2, the Pt microelectrode was voltammetry cycled in 0.1 M sulfuric acid with the potential from −1.5 to 1.5 V for 30 cycles.

The cleaned Pt wire microelectrode was potential scanned in GO aqueous suspension (0.1 M carbonate buffer at pH 9.0) containing H_2PtCl_6 under the potential window from 0 to −1.5 V at a scan rate of 25 mV s^{-1}. The resulted PtNF/ERGO/Pt wire electrode was rinsed by deionized water and dried by nitrogen. Then it was wrapped with insulating tape, leaving 2 mm in length for sensing.

The ERGO/Pt and PtNF/Pt electrode was also prepared in 0.1 M carbonate buffer contain optimal concentrations of GO or H_2PtCl_6 for control.

2.3. Characterization

The surface morphology of the different modified Pt wire electrodes were characterized by scanning electron microscopic (SEM,

JEOL JSM-6700F). The X-ray diffraction (XRD) analysis of the different modified Pt electrode was carried out on a SmartLab XRD system using Cu Kα as the radiation source at an operating voltage of 40 kV. Pt sheet was used as the substrate to simulate the Pt wire.

2.4. Preparation of plant samples and homogenate

A homogenous seeds of sunflower (LD5009) were obtained from Beijing Kafry Technology Co., LTD. After seed germination, the seedlings with consistent growth were selected and transplanted into half-strength Hoagland solution. After 15 days hydroponic culture in an illuminating incubator (10 h/14 h of light/dark period, 25 ± 2 °C and 60% humidity), the sunflowers were randomized into three groups (each group contained 20 plant samples) and treated by different salt stress for 10 h through introducing different levels of NaCl (0, 50 and 100 mM) into the Hoagland solution.

Homogenates of stems of sunflower seedling was prepared by homogenized the plant materials thoroughly with 0.5 g of crystalline silica. The homogenates were centrifuged at 10 000 rpm (10 min, 4 °C), and the supernatant solutions were collected and transferred to new tubes. The homogenates were prepared freshly before each measurement.

2.5. Electrochemical measurements

All the electrochemical experiments were performed on a CHI 760e electrochemical working station. A two-electrode system was employed for the measurements. The modified Pt microelectrode was used as working electrode. A Ag/AgCl wire was used as reference/counter electrode, which was prepared by chloridizing Ag wire at 0.6 V in 0.1 M hydrochloride acid for about 30 min. Cyclic voltammetry (CV) was conducted from 0.6 V to 1.4 V at 50 mV s^{-1}. Differential pulse voltammetry (DPV) was conducted from 0.6 V to 1.4 V, and the parameters were: 0.02 V of increasing potential, 0.02 s of pulse width, 0.05 V of amplitude, 1 s of pulse period, and 0.02 s of sampling width.

For *in vivo* detection of SA in the stem of sunflower seedlings, the stem of the seedlings were punched with a puncture needle to obtain two holes. The working electrode and Ag/AgCl electrode were placed into the holes respectively. For different plant, the electrode was placed approximately the same site as possible.

2.6. Ultra-performance liquid chromatography-mass spectrometric (UPLC-MS) measurements

For the UPLC-MS (Water Acquity I-Class, Waters Corporation, MA, US; Thermo Q-Exactive, Thermo Scientific, MA, US) measurements, the stem samples of the seedlings were collected and ground in liquid nitrogen immediately after 10 hours salt treatments. 1 g of ground sample was added 2 ml 4 °C precooled methanol (80%) and extracted overnight at 4 °C. The extract was mixed with 1 ml of $CHCl_3$. Then the solution was vibrated at 900 rpm for 4 min at 4 °C. After centrifuging at 14 000 rpm for 5 min at 4 °C, the supernatant was collected and dried by nitrogen at room temperature. The prepared sample was dissolved in 1 mL of methanol and filtrated by a 0.22 μm microporous membrane before UPLC-MS measurements.

2.7. Gene expression analysis

To confirm the result of *in vivo* detection of SA, semi quantitative RT-PCR analysis was performed for SA-related gene *def* and *HaAC1*. Total RNA was extracted from stem samples of sunflower seedlings (0.1 g fresh weight) with OminiPlant RNA Kit (DNase I) (ComWin Biotech, Beijing, China) according to the protocols. BioRT cDNA First Strand Synthesis Kit (Bioer, Hangzhou, China) was used to synthesis the first-strand cDNAs from 2 μg total RNA. RT-PCR was performed with 1 μL generated cDNA. PCR amplifications conditions: initial denaturation, 95 °C for 5 min; 30 cycles of amplification, 94 °C (30 s), 58 °C (40 s), and 72 °C (40 s); final extension, 72 °C for 7 min. 6 μL of the PCR product was separated on agarose gel (1.5%).

The primers used for *def* were: F: 5′-GTGAGAAGG CAAGCCAGACA-3′ and R: 5′-TCAAGGTTTGGCTGTCGCCT-3′ (AF364865, referred to Hu *et al.*, 2003).[20] The primers used for *HaAC1* were: F: 5′-CACCACCAGGGAAATGATG-3′ and R: 5′-TGCGGACAACTGAGAACAACA-3′ (AF030301). G-Marker (EU112625) (F: 5′-GCTGTGGCCCTTGTGTTG-3′ and R: 5′-CGCAGACCGATAGGATACCATT-30) was used as control for the comparison of amounts of cDNA in each reaction.

3. Result and discussion

3.1. Characterization of the PtNF/ERGO/Pt microelectrodes

The surface morphology of electrodes was characterized by SEM. As shown in Fig. 1A, the surface of the bare Pt microelectrode is smooth and clean. When the ERGO was formed on the Pt microelectrode (Fig. 1B), the typical crumpled and wrinkled structure of ERGO can be observed. When the PtNF was formed on the Pt microelectrode (Fig. 1C), a densely and uniformly distributed flower-like Pt nanostructure with the diameter of 200–500 nm can be observed. When the Pt and GO was co-deposition and co-reduction on the Pt microelectrode, flower-like Pt nanostructure are dispersed in the lamellar ERGO, constructing a porous network structure (Fig. 1D). The diameters of the PtNF range from 50–100 nm. It has been reported that GO or RGO can be used to disperse and prevent the growth of the nanostructures, because they could be regarded as unconventional polymeric surfactant,[21–23] so smaller size and better dispersion were observed for the PtNF with the attendance of ERGO. And ERGO can also provide anchoring site for metal nanostructures or its precursors.[24,25] Moreover, the irregularly shaped PtNF and untidy ERGO can enhance the surface area and catalytic activity of the Pt microelectrode greatly.[2,26]

The XRD pattern of (a) bare Pt, (b) EGRO/Pt, (c) Pt NF/Pt and (d) Pt NF/EGRO/Pt was shown in Fig. 1E. For the bare Pt (a), the peaks at 2θ of 39.8°, 46.3°, and 67.8° are assigned to the (111), (200), and (220) planes of the Pt particles. The peak at 2θ of 67.8° is very strong, which might be ascribed to the preferred orientation of block as we used the Pt sheet to simulate the Pt wire. For the EGRO/Pt (b), a weak peak originating from graphene sheets (002) is also appeared at 2θ of about 25°, which confirms the reduction of GO into ERGO.[27] For the Pt NF/Pt (c), the intensity of peaks of 39.8°, 46.3°, and 67.8° are changed compare to the bare Pt sheet (a), indicating the formation of Pt crystals.[28] As expected, a peak at 2θ of 25° also appears for the Pt NF/EGRO/Pt.

3.2. Feasibility of the PtNF/ERGO/Pt microelectrode for detecting SA

The feasibility of the modified PtNF/ERGO/Pt microelectrode for detecting SA was tested by cyclic voltammetry (CV) and
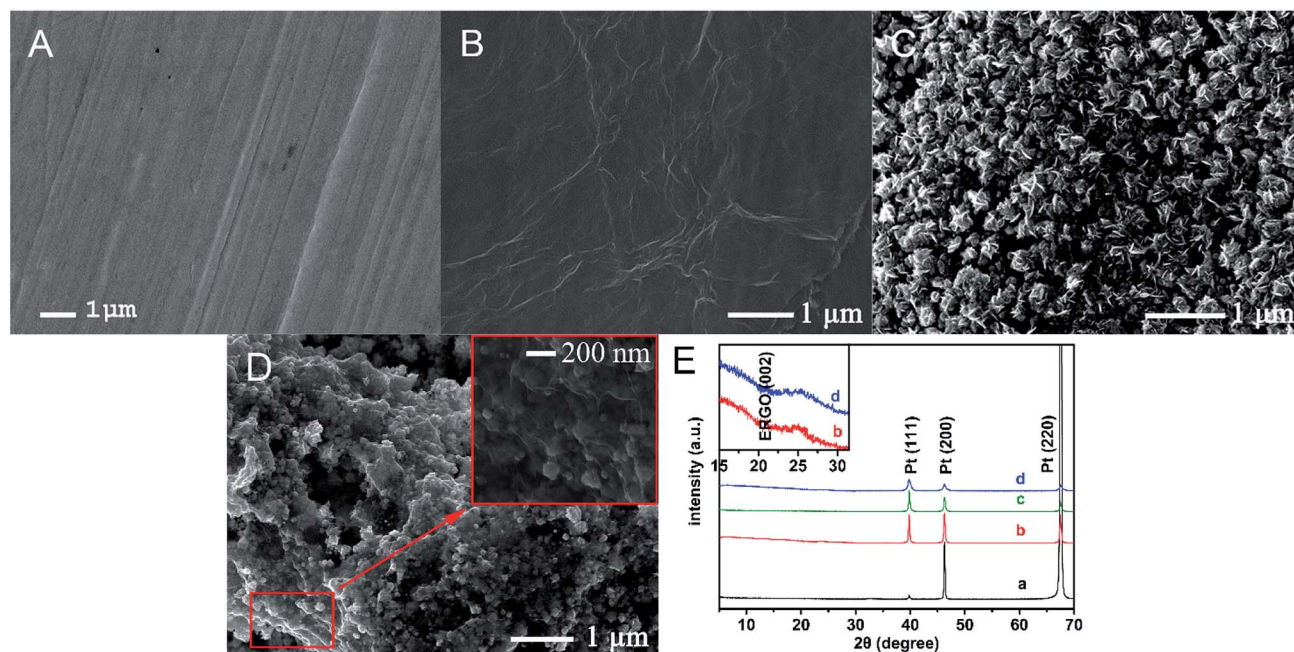

Fig. 1 SEM images of the bare Pt electrode (A), ERGO/Pt electrode (B), PtNF/Pt electrode (C), and the PtNF/ERGO/Pt electrode (D), the insert is a partial enlargement of the PtNF/ERGO/Pt electrode. (E) XRD patterns of (a) bare Pt sheet, (b) ERGO/Pt, (c) PtNF/Pt, (d) PtNF/ERGO/Pt.
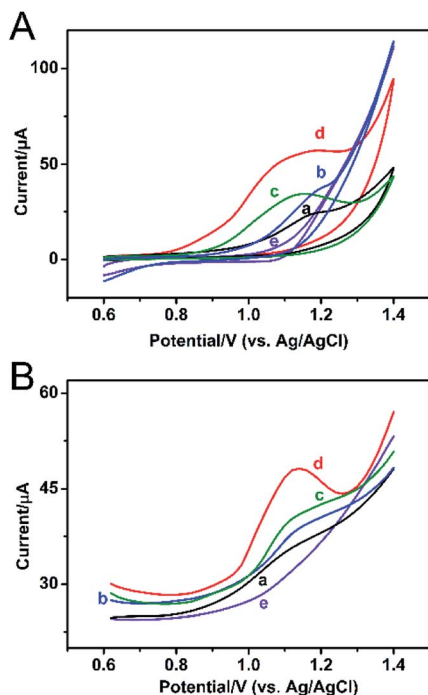
Fig. 2 (A) CV and (B) DPV curves of the bare Pt electrode (a), ERGO/Pt electrode (b), PtNF/Pt electrode(c), PtNF/ERGO/Pt electrode (d) in the presence of 500 μM SA, and the PtNF/ERGO/Pt electrode (e) in the PBS without SA.

differential pulse voltammetry (DPV) methods. For CV curve of 500 μM SA (Fig. 2A), a single oxidation peak appeared around 1.15 V by the bare Pt microelectrode in the PBS buffer (curve a), which is probably attributed to the electrochemically active phenol group of SA.[11] The oxidation peak was increased when the ERGO/Pt microelectrode (curve b) and the PtNF/Pt microelectrode (curve c) were used, indicating the PtNF and ERGO can respectively enhanced the catalysis effect of SA. The oxidation peak of SA was significantly increased when the PtNF/ERGO/Pt microelectrode was used (curve d), indicating that the integration of high density Pt NF with the layered ERGO can induce more active sites and construct an electrical network, which greatly increased the catalytic capacity to SA. No oxidation peak was observed in the absence of SA using the PtNF/ERGO/Pt microelectrode (curve e). In the DPV curve (Fig. 2B), similar trends as that of CV curves were observed for the

different modified electrodes. An oxidation peak with much higher peak height also appeared at the similar potential for the PtNF/ERGO/Pt microelectrode in the presence of SA (Fig. 2B, curve e).

3.3. Optimization of conditions for detection in solution

The concentration of GO and $H_2PtCl_6 \cdot 6H_2O$ and the scan cycles of electrodeposition were optimized as they are the key factors in the electrodeposition process. As shown in Fig. 3A, with the increase of the concentration of GO from 0 to 1 mg ml^{-1}, the peak current of SA increases. While further increasing the concentration of GO, the peak current of SA decreases. So the optimal concentration of GO is 1 mg ml^{-1}. The optimal conditions for $H_2PtCl_6 \cdot 6H_2O$ and scan cycles are 10 mM and 45 cycles respectively as can be seen from Fig. 3B and C.

3.4. Performance of PtNF/ERGO/Pt microsensor

The modified electrode was used to detect different concentrations of SA standard solution using DPV method. As shown in Fig. 4A, with the increasing concentrations of SA, the peak current of SA increases correspondingly. There is a decent linear relation between the peak currents and the logarithm value of the concentrations of SA from 100 pM to 1 μM (Fig. 4B). And the equation is I_{peak} (μA) = $0.45LNC_{SA}$ (nM) + 1.05, the correlation coefficient is 0.9807. The detection limit of this sensor is 48.11 pM (S/N = 3.0). The sensing performance of the PtNF/ERGO/Pt microsensor for SA is compared with the previous reports. As shown in Table S1,† the developed sensor in this work is superior to most electrochemical sensors existed for SA.[2,11,29–33]

Selectivity is an important parameter to evaluate the performance of the sensor. Therefore, the possible interference in the seedling stem sap was examined by the proposed sensor under the same condition. As shown in Fig. 5, an oxidation peak around 1.15 V is observed for SA. Besides, a weak peak near +0.8 V is observed for indole-3-acetic acid with the same concentration, which is consistent with previous report.[11] However, it does not interfere with the detection of SA. Other components including malic acid, citric acid, succinic acid, abscisic acid and methyl jasmonate don't show any responses in the DPV curve. This result suggests the high selectivity of the proposed microsensor. The RSD was 15% for 8 different PtNF/
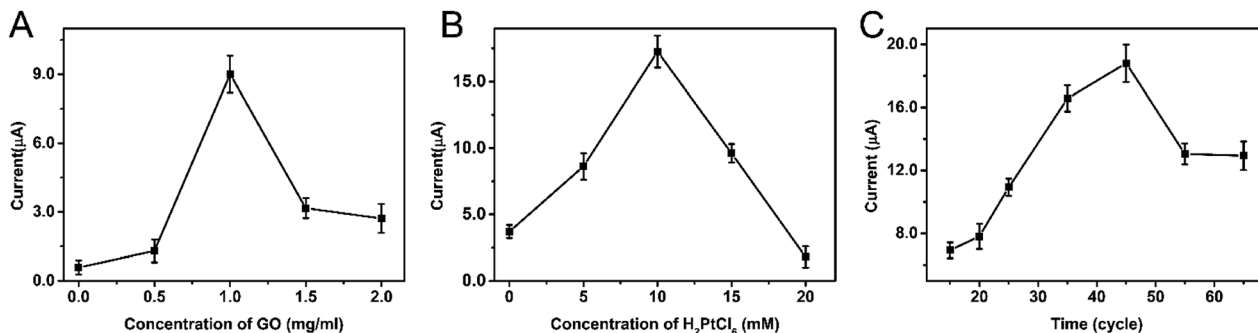

Fig. 3 Optimization of the modification process with different concentrations of GO (A), H_2PtCl_6 (B), and different scan cycles for deposition (C).
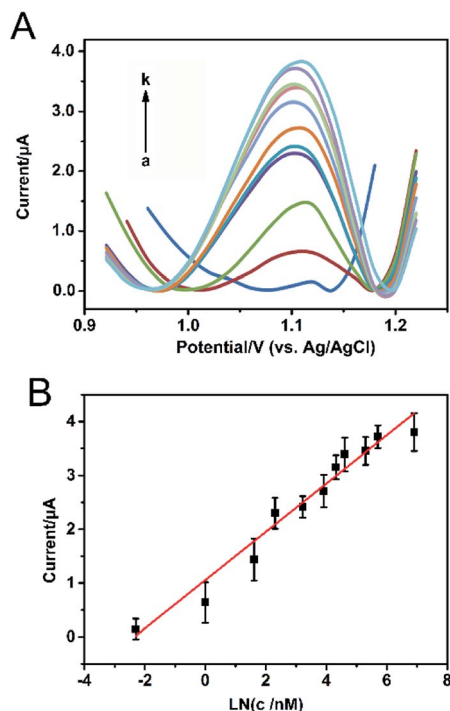
Fig. 4 (A) DPV curves of SA with concentrations of 0.1, 1.0, 5.0, 10.0, 25.0, 50.0, 75.0, 100.0, 200.0, 300.0, 1000 nM (from a to k in turn) detected by the PtNF/ERGO/Pt electrode. (B) The calibration curve of the DPV peak current and the logarithm value of SA concentrations in PBS buffer. The average values and standard deviations were obtained based on five results.

ERGO/Pt microelectrodes in the presence of 500 μM SA. There is still 86% sensing ability remained for the microsensor after storage at 4 °C for three weeks, indicating that this microsensor is highly stable.

In order to obtain a standard curve which is more suitable to be applied in the living plants,[34] the DPV responses of modified electrode for SA was also detected in 10% homogenate of sunflower stems diluted by 0.1 M PBS (Fig.S1†). As shown in Fig. 6, the linear equation is I'_{peak} (μA) = 0.088LNC'_{SA} (nM) + 0.993 for SA from 10 pM to 500 nM. The detection limit is 3.3 pM (at S/N of 3.0), and correlation coefficient is 0.9811.

3.5. *In vivo* measurements of SA in sunflower seedlings under salt stress

Salt stress is one of the major abiotic environmental factors which adversely affect plant growth and development. Phytohormones play critical roles in regulating plant responses to salt stress.[35] In this work, the modified PtNF/ERGO/Pt microelectrode was used to detect the SA levels *in vivo* in sunflower seedlings under different salt stress. Fig. 7A is the photograph for the *in vivo* detection of SA in sunflower seedlings. Fig. 7B shows the typical DPV results for the *in vivo* detection of SA in sunflower seedlings. The concentration of SA in the stem part of sunflowers is 256.1 ± 0.32 nM, 179.5 ± 0.25 nM, and 158.6 ± 0.15 nM for 0 mM, 50 mM and 100 mM of NaCl treatments (10 h), respectively, according to the standard curve in 10% homogenate of sunflower stems. This result suggests that with the increasing concentrations of salt, the SA levels decreases. This result is consistent with previous studies.[31,36] In addition, the diameter of the microelectrode is only 0.5 mm, only tiny holes were left after the detection. And the electrochemical test is so fast that there is no much influences were observed on the following growth of the plants.

In order to verify our result, UPLC-MS method was used to measure the SA levels in the extracted samples of the stem part of sunflower seedlings after different treatment of salt stress. The obtained result is shown in Fig. 7C, it could be found that the trend of SA levels is decreased with the increasing concentrations of salt, which is consistent with those obtained by the proposed electrochemical sensor.

The expression of SA related gene in sunflowers was also analyzed by RT-PCR method. The product of *def* is defensin (PR12 protein). It is a kind of antifungus, which can be impacted by SA.[20] *HaAC1* encodes aldoketo reductase, which also is a marker of SA pathway in sunflowers.[37] As shown in Fig. 7D, the expression of *HaAC1* gene is down-regulated with the increasing concentrations of salt. The expression of *def* gene is slightly up-regulated for the salt-treated groups, but for the 50 mM and 100 mM of salt treatment, the expression change of *def* gene is not obvious. Similar trend of SA levels and the expression of *def* and *HaAC1* gene are also observed for sunflowers when it was attacked by *Orobanche Cumana*.[20]
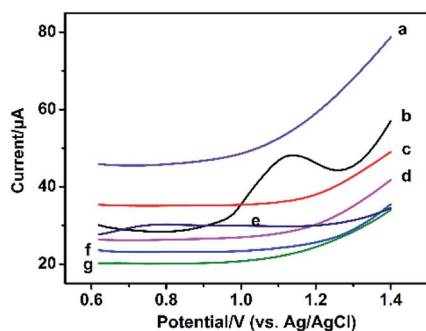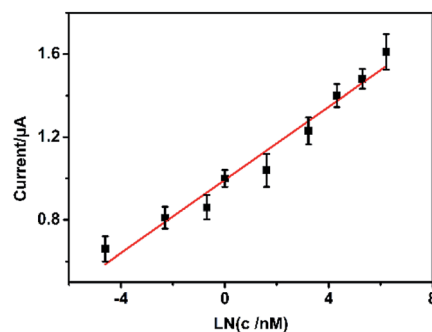

Fig. 5 DPV responses of 500 μM methyl jasmonate (a), malic acid (c), succinic acid (d), indole-3-acetic acid (e), citric acid (f), abscisic acid (g), and salicylic acid (b) detected by the PtNF/ERGO/Pt electrode.

Fig. 6 The calibration curve of the DPV peak current and the logarithm of SA concentrations (0.01, 0.1, 0.5, 1.0, 5.0, 25.0, 75.0, 200.0, 500.0 nM in turn) in a 10% homogenate of sunflower seedling stems diluted by 0.01 M PBS.
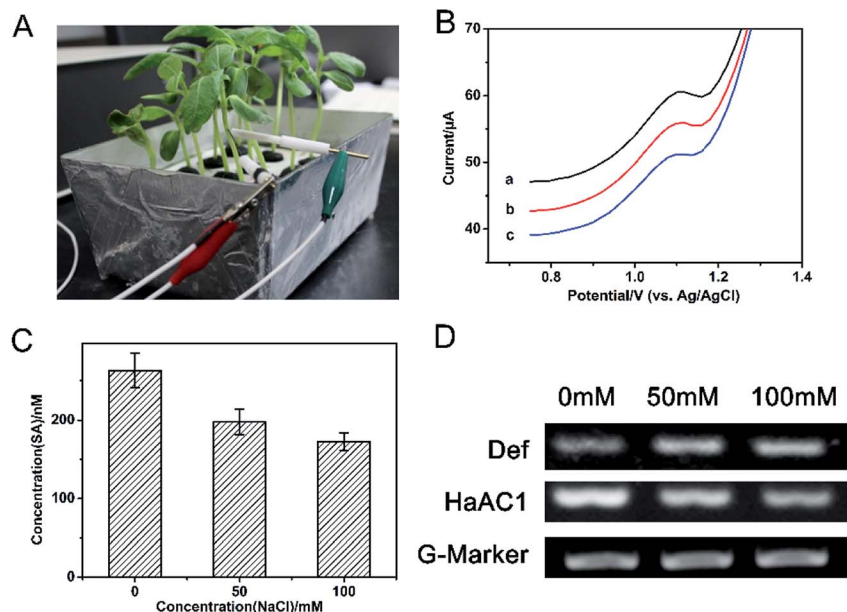
Fig. 7 (A) The real image of *in vivo* detection of SA in a sunflower seedling stem by the PtNF/ERGO/Pt electrode. (B) Typical DPV curves for the *in vivo* detection of SA by the PtNF/ERGO/Pt electrode under different salt stress: 0 mM (a), 50 mM (b) and 100 mM (c). (C) UPLC-MS result of SA levels in the stem of sunflower seedlings. (D) Gene expression analysis of *def*, *HaAC1* gene relative to G-Marker in the stem of sunflower seedlings.

4.   Conclusions

In summary, the PtNF/ERGO/Pt microelectrode was developed to detect SA in the stem of sunflower seedlings under different salt stress *in vivo*. Our result was consistent with previous report, and also confirmed by UPLC-MS and gene expression analysis. This is the first time for *in vivo* detection of SA in plants using microelectrode. The proposed SA microsensor is simple and practical, and showed high sensitivity and selectivity. It is foreseeable that our strategy could pave the way for the *in vivo* detection of phytohormone in plants.

Conflicts of interest

There are no conflicts to declare.

Acknowledgements

Notes and references

1 B. Lacombe and P. Achard, *Curr. Opin. Plant Biol.*, 2016, **34**, 1–8.

2 Z. Wang, F. Ai, Q. Xu, Q. Yang, J. H. Yu, W. H. Huang and Y. D. Zhao, *Colloids Surf., B*, 2010, **76**, 370–374.

3 S. Hayat, A. Ahmad and M. N. Alyemeni, *Salicylic acid: plant growth and development*, Springer, Netherlands, 2013.

4 S. Croubels, M. An, K. Baert and P. D. Backer, *Anal. Chim. Acta*, 2005, **529**, 179–187.

5 R. A. Budi Muljono, A. M. G. Looman, R. Verpoorte and J. J. C. Scheffer, *Phytochem. Anal.*, 2015, **9**, 35–38.

6 J. Sun, B. Wang, Z. Xue, Z. Li and X. Yang, *Anal. Chem.*, 2016, **88**, 1355–1361.

7 M. M. Sena, M. G. Trevisan and R. J. Poppi, *Talanta*, 2006, **68**, 1707–1712.

8 P. J. Tseng, C. Y. Wang, T. Y. Huang, Y. Y. Chuang, S. F. Fu and Y. W. Lin, *Anal. Methods*, 2014, **6**, 1759–1765.

9 W. Huang, L. Huang, G. Preston, M. Naylor, J. Carr, Y. Li, A. Singer, A. Whiteley and H. Wang, *Plant J.*, 2010, **46**, 1073–1083.

10 M. I. Gonzálezsánchez, P. T. Lee, R. H. Guy and R. G. Compton, *Chem. Commun.*, 2015, **51**, 16534–16536.

11 L. Sun, Q. Feng, Y. Yan, Z. Pan, X. Li, F. Song, H. Yang, J. Xu, N. Bao and H. Gu, *Biosens. Bioelectron.*, 2014, **60**, 154–160.

12 Y. Liu, G. Sun, C. Jiang, X. Zheng, L. Zheng and C. Li, *Microchim. Acta*, 2014, **181**, 63–70.

13 Y. Ning, Y. Chen, Y. Shen, Y. Tang, J. Guo, F. Fang and S. Liu, *J. Electrochem. Soc.*, 2013, **160**, H715–H719.

14 Q. Xu, F. Wei, Z. Wang, Q. Yang, Y. D. Zhao and H. Chen, *Sens. Actuators, B*, 2009, **141**, 599–603.

15 Q. Q. Ren, X. R. Huang, G. C. Liu, J. Ou-Yang, M. T. Li, H. Chen, Y. D. Zhao and W. Chen, *Sens. Actuators, B*, 2015, **220**, 743–748.

16 Q. Xu, F. Wei, Z. Wang, Q. Yang, Y. D. Zhao and H. Chen, *Phytochem. Anal.*, 2010, **21**, 192–196.

17 A. S. Lima, K. R. Prieto, C. S. Santos, V. H. Paula, E. Y. Garciaochoa, A. Huertarobles, M. J. Beltrangarcia, M. P. Di and M. Bertotti, *Biosens. Bioelectron.*, 2018, **99**, 108–114.

18 A. L. Liu, G. X. Zhong, J. Y. Chen, S. H. Weng, H. N. Huang, W. Chen, L. Q. Lin, Y. Lei, F. H. Fu and Z. L. Sun, *Anal. Chim. Acta*, 2013, **767**, 50–58.

19 H. Gao, F. Xiao, B. C. Chi and H. Duan, *ACS Appl. Mater. Interfaces*, 2011, **3**, 3049–3057.

20 X. Hu, D. L. Bidney, N. Yalpani, J. P. Duvick, O. Crasta, O. Folkerts and G. Lu, *Plant Physiol.*, 2003, **133**, 170–181.

21 C. Liu, K. Wang, S. Luo, Y. Tang and L. Chen, *Small*, 2011, **7**, 1203–1206.

22 J. Yang, C. Tian, L. Wang and H. Fu, *J. Mater. Chem.*, 2011, **21**, 3384–3390.

23 M. Zhu, P. Chen and M. Liu, *Langmuir*, 2012, **28**, 3385–3390.

24 C. V. Rao, A. L. M. Reddy, Y. Ishikawa and P. M. Ajayan, *Carbon*, 2011, **49**, 931–936.

25 C. V. Rao, C. R. Cabrera and Y. Ishikawa, *J. Phys. Chem. C*, 2011, **115**, 21963–21970.

26 Y. Hu, P. Wu, H. Zhang and C. Cai, *Electrochim. Acta*, 2012, **85**, 314–321.

27 L. J. Cote, R. Cruzsilva and J. Huang, *J. Am. Chem. Soc.*, 2009, **131**, 11027–11032.

28 Y. Si and E. T. Samulski, *Chem. Mater.*, 2008, **20**, 6792–6797.

29 L. Lu, X. Zhu, X. Qiu, H. He, J. Xu and X. Wang, *Int. J. Electrochem. Sci.*, 2014, **9**, 8057–8066.

30 J. Park and C. Eun, *Electrochim. Acta*, 2016, **194**, 346–356.

31 L. Sun, X. Liu, L. Gao, Y. Lu, Y. Li, Z. Pan, N. Bao and H. Gu, *Anal. Lett.*, 2015, **48**, 1578–1592.

32 Z. Wang, F. Wei, S. Y. Liu, Q. Xu, J. Y. Huang, X. Y. Dong, J. H. Yu, Q. Yang, Y. D. Zhao and H. Chen, *Talanta*, 2010, **80**, 1277–1281.

33 M. H. A. Zavar, S. Heydari and G. H. Rounaghi, *Arabian J. Sci. Eng.*, 2013, **38**, 29–36.

34 W. Chen, Q. Yang, Q. Q. Ren, W. Wen, D. H. Jiang and Y. D. Zhao, *Nanosci. Nanotechnol.*, 2013, **5**, 694–698.

35 A. Molina and J. P. Donaire, *New Phytol.*, 2010, **156**, 409–415.

36 M. G. Javid, A. Sorooshzadeh, F. Moradi, S. A. M. M. Sanavy and I. Allahdadi, *Aust. J. Crop Sci.*, 2011, **5**, 726–734.

37 P. Letousey, A. De Zélicourt, D. S. C. Vieira, S. Thoiron, F. Monteau, P. Simier, P. Thalouarn and P. Delavault, *Plant Pathol.*, 2007, **56**, 536–546.